

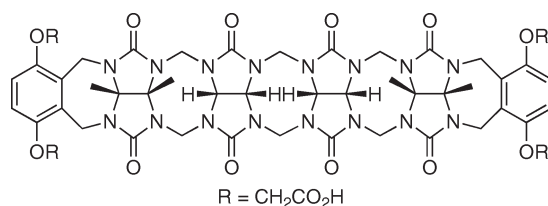
Acyclic Cucurbit[*n*]uril Congeners Are High Affinity Hosts

Da Ma, Peter Y. Zavalij, and Lyle Isaacs*

Department of Chemistry and Biochemistry, University of Maryland, College Park, Maryland 20742

lisaacs@umd.edu

Received April 19, 2010



We present the design, synthesis via methylene bridged glycoluril tetramer building blocks, and characterization of acyclic cucurbit[*n*]uril congeners that function as hosts for a wide variety of ammonium ions in water. The X-ray crystallographic characterization of the free host and its complexes with *p*-xylylenediamine and spermine establish the flexibility of the methylene bridged backbone of the acyclic cucurbit[*n*]uril congeners that allow them to adapt to the structural features of the guest. We find that the acyclic cucurbit[*n*]uril congeners—with their four contiguous methylene bridged glycoluril units and two aromatic *o*-xylylene walls bearing CO₂H substituents—bind to ammonium ions in buffered water with values of K_a ranging from $\sim 10^5 \text{ M}^{-1}$ to greater than 10^9 M^{-1} . Similar to the cucurbit[*n*]uril family of hosts, we find that increasing the concentration of metal cations in the buffer reduces the affinity of the acyclic cucurbit[*n*]uril congener toward guests by competitive binding at the ureidyl C=O portals. Although the acyclic cucurbit[*n*]uril congeners retain the ability to bind to ammonium ions with high affinity, they do so with lower selectivity than cucurbit[*n*]urils presumably do to the structural flexibility of the hosts. A methylene bridged glycoluril tetramer model compound that lacks the substituted *o*-xylylene walls is a much lower affinity host, which establishes the importance of these rings on the overall recognition behavior of the acyclic cucurbit[*n*]uril congeners. Overall, the results in this paper establish that acyclic cucurbit[*n*]uril receptors that contain four or more contiguous methylene bridged glycoluril units retain many of the excellent recognition properties of the cucurbit[*n*]uril family.

Introduction

The cucurbit[*n*]uril (CB[*n*], $n = 5, 6, 7, 8, 10$) family of molecular containers (Chart 1) are formed in a single step by the condensation of glycoluril with formaldehyde under strongly acidic conditions.¹ The key structural features of CB[*n*] molecular containers are the presence of a hydrophobic cavity guarded by two symmetry equivalent ureidyl carbonyl portals

that constitute regions of high negative electrostatic potential.^{2,3}

As a consequence of these structural features CB[*n*] compounds bind to species that contain both hydrophobic chains and cationic groups (Chart 1). In a series of elegant papers throughout the 1980s Mock showed that CB[6] displays tight and highly selective binding interactions toward alkaneammonium and alkanediammonium ions in aqueous solution and used these properties to catalyze a 3+2 dipolar cycloaddition and construct an early example of a molecular switch.^{4,5} Interest in the CB[*n*] family of molecular containers surged after the isolation of the larger CB[*n*] homologues that displayed even more interesting recognition properties. For example, the exceptionally high

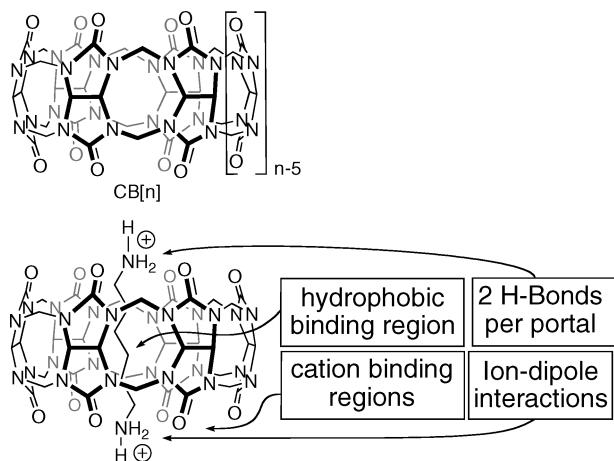
(1) Day, A.; Arnold, A. P.; Blanch, R. J.; Snushall, B. *J. Org. Chem.* **2001**, *66*, 8094–8100. Freeman, W. A.; Mock, W. L.; Shih, N.-Y. *J. Am. Chem. Soc.* **1981**, *103*, 7367–7368. Kim, J.; Jung, I.-S.; Kim, S.-Y.; Lee, E.; Kang, J.-K.; Sakamoto, S.; Yamaguchi, K.; Kim, K. *J. Am. Chem. Soc.* **2000**, *122*, 540–541. Liu, S.; Zavalij, P. Y.; Isaacs, L. *J. Am. Chem. Soc.* **2005**, *127*, 16798–16799.

(2) Lagona, J.; Mukhopadhyay, P.; Chakrabarti, S.; Isaacs, L. *Angew. Chem., Int. Ed.* **2005**, *44*, 4844–4870.

(3) Lee, J. W.; Samal, S.; Selvapalam, N.; Kim, H.-J.; Kim, K. *Acc. Chem. Res.* **2003**, *36*, 621–630.

(4) Mock, W. L.; Irra, T. A.; Wepsiec, J. P.; Adhya, M. *J. Org. Chem.* **1989**, *54*, 5302–5308. Mock, W. L.; Shih, N.-Y. *J. Am. Chem. Soc.* **1988**, *110*, 4706–4710.

(5) Mock, W. L.; Shih, N.-Y. *J. Org. Chem.* **1986**, *51*, 4440–4446.

CHART 1. Structure of CB[n] Molecular Containers and the CB[6]·Hexanediammonium Ion Complex

binding constants (K_a up to 10^{15} M^{-1}) displayed by CB[7]^{6,7} and the ability of CB[8] and CB[10] to bind two guests simultaneously has resulted in a number of intriguing applications including the preparation of molecular machines,⁸ chemical sensors, stationary phases for chromatographic separations and affinity capture, supramolecular polymers, supramolecular catalysis, and drug delivery vehicles.^{2,3,9}

Despite the range of applications demonstrated for members of the CB[n] family, a number of issues have not been fully resolved that currently limit an even wider application of the CB[n] family.² The first issue is the generally poor solubility

characteristics of CB[6], CB[8], and CB[10] ($< 100 \mu\text{M}$) in D_2O . A second, related issue is that the preparation of CB[n] derivatives, especially those with enhanced solubility, is challenging, particularly for the higher CB[n] homologues ($n = 7, 8, 10$).¹⁰ A final issue involves the dynamics of the formation and dissociation of CB[n] complexes. Because of their narrow ureidyl carbonyl portals, CB[n] compounds exhibit constrictive binding.^{11,12} In constrictive binding processes, large barriers to dissociation and sometimes association translate into kinetics of dissociation and association that are slow on the laboratory time scale. Obviously, slow kinetics can be a limitation in many applications.

Over the past decade we have been using mechanistic insights to guide us toward synthetic approaches that alleviate some of these limitations. In one line of inquiry we have used glycoluril surrogates to prepare CB[n] analogues with built-in fluorescent walls.^{13,14} In a second line of inquiry we have starved the CB[n] forming reaction of formaldehyde and isolated acyclic glycoluril oligomers and a number of macrocyclic CB[n]-type compounds lacking one or more bridging CH_2 groups (known as *nor-seco*-CB[n]).^{15–17} In a third line of inquiry we have appended *o*-xylylene walls to glycoluril dimers and related systems and delineated the recognition properties (e.g., enantiomeric self-recognition, heterochiral recognition, and self-sorting) of the resultant acyclic CB[n] congeners.^{18–20} Recently, Sindelar has reported the synthesis and recognition properties of a glycoluril trimer capped with *o*-xylylene rings.²¹ Throughout these studies we have found that any structural change that compromised the highly electrostatically negative ureidyl carbonyl portals decreased the affinity of host toward guest. In this paper we continue the third line of inquiry by using building blocks **1–4** to prepare hosts **5a** and **5b** that comprise a methylene bridged glycoluril tetramer capped with two substituted *o*-xylylene rings and control compound **6** that

(6) Liu, S.; Ruspic, C.; Mukhopadhyay, P.; Chakrabarti, S.; Zavalij, P. Y.; Isaacs, L. *J. Am. Chem. Soc.* **2005**, *127*, 15959–15967.

(7) Rekharsky, M. V.; Mori, T.; Yang, C.; Ko, Y. H.; Selvapalam, N.; Kim, H.; Sobransingh, D.; Kaifer, A. E.; Liu, S.; Isaacs, L.; Chen, W.; Moghaddam, S.; Gilson, M. K.; Kim, K.; Inoue, Y. *Proc. Natl. Acad. Sci. U.S.A.* **2007**, *104*, 20737–20742. Jeon, W. S.; Moon, K.; Park, S. H.; Chun, H.; Ko, Y. H.; Lee, J. Y.; Lee, E. S.; Samal, S.; Selvapalam, N.; Rekharsky, M. V.; Sindelar, V.; Sobransingh, D.; Inoue, Y.; Kaifer, A. E.; Kim, K. *J. Am. Chem. Soc.* **2005**, *127*, 12984–12989.

(8) Ko, Y. H.; Kim, E.; Hwang, I.; Kim, K. *Chem. Commun.* **2007**, 1305–1315.

(9) Hennig, A.; Bakirci, H.; Nau, W. M. *Nat. Methods* **2007**, *4*, 629–632. Praetorius, A.; Bailey, D. M.; Schwarzlose, T.; Nau, W. M. *Org. Lett.* **2008**, *10*, 4089–4092. An, Q.; Li, G.; Tao, C.; Li, Y.; Wu, Y.; Zhang, W. *Chem. Commun.* **2008**, 1989–1991. Angelos, S.; Khashab, N. M.; Yang, Y.-W.; Trabolsi, A.; Khatib, H. A.; Stoddart, J. F.; Zink, J. I. *J. Am. Chem. Soc.* **2009**, *131*, 12912–12914. Angelos, S.; Yang, Y.-W.; Patel, K.; Stoddart, J. F.; Zink, J. I. *Angew. Chem., Int. Ed.* **2008**, *47*, 2222–2226. Bali, M. S.; Buck, D. P.; Coe, A. J.; Day, A. I.; Collins, J. G. *Dalton Trans.* **2006**, 5337–5344. Baumes, L. A.; Sogo, M. B.; Montes-Navajas, P.; Corma, A.; Garcia, H. *Tetrahedron Lett.* **2009**, *50*, 7001–7004. Bush, M. E.; Bouley, N. D.; Urbach, A. R. *J. Am. Chem. Soc.* **2005**, *127*, 14511–14517. Chakrabarti, S.; Mukhopadhyay, P.; Lin, S.; Isaacs, L. *Org. Lett.* **2007**, *9*, 2349–2352. Hwang, I.; Ziganshina, A. Y.; Ko, Y.-H.; Yun, G.; Kim, K. *Chem. Commun.* **2009**, 416–418. Kemp, S.; Wheate, N. J.; Pisani, M. J.; Aldrich-Wright, J. R. *J. Med. Chem.* **2008**, *51*, 2787–2794. Lee, J. W.; Hwang, I.; Jeon, W. S.; Ko, Y. H.; Sakamoto, S.; Yamaguchi, K.; Kim, K. *Chem. Asian J.* **2008**, *3*, 1277–1283. Montes-Navajas, P.; Baumes, L. A.; Corma, A.; Garcia, H. *Tetrahedron Lett.* **2009**, *50*, 2301–2304. Nagarajan, E. R.; Oh, D. H.; Selvapalam, N.; Ko, Y. H.; Park, K. M.; Kim, K. *Tetrahedron Lett.* **2006**, *47*, 2073–2075. Park, K. M.; Suh, K.; Jung, H.; Lee, D.-W.; Ahn, Y.; Kim, J.; Baek, K.; Kim, K. *Chem. Commun.* **2009**, 71–73. Saleh, N.; Koner, A. L.; Nau, W. M. *Angew. Chem., Int. Ed.* **2008**, *47*, 5398–5401. Sindelar, V.; Silvi, S.; Kaifer, A. E. *Chem. Commun.* **2006**, 2185–2187. Sindelar, V.; Silvi, S.; Parker, S. E.; Sobransingh, D.; Kaifer, A. E. *Adv. Funct. Mater.* **2007**, *17*, 694–701. Sun, S.; Zhang, R.; Andersson, S.; Pan, J.; Zou, D.; Akermark, B.; Sun, L. *J. Phys. Chem. B* **2007**, *111*, 13357–13363. Tuncel, D.; Oezsar, O.; Tiftik, H. B.; Salih, B. *Chem. Commun.* **2007**, 1369–1371. Wu, J.; Isaacs, L. *Chem.—Eur. J.* **2009**, *15*, 11675–11680. Zhao, Y.; Buck, D. P.; Morris, D. L.; Pourgholami, M. H.; Day, A. I.; Collins, J. G. *Org. Biomol. Chem.* **2008**, *6*, 4509–4515. Rauwald, U.; Scherman, O. A. *Angew. Chem., Int. Ed.* **2008**, *47*, 3950–3953. Ghosh, S.; Isaacs, L. *J. Am. Chem. Soc.* **2010**, *132*, 4445–4454.

(10) Jon, S. Y.; Selvapalam, N.; Oh, D. H.; Kang, J.-K.; Kim, S.-Y.; Jeon, Y. J.; Lee, J. W.; Kim, K. *J. Am. Chem. Soc.* **2003**, *125*, 10186–10187.

(11) Mock, W. L.; Shih, N.-Y. *J. Am. Chem. Soc.* **1989**, *111*, 2697–2699. Marquez, C.; Nau, W. M. *Angew. Chem., Int. Ed.* **2001**, *40*, 3155–3160. Pluth, M. D.; Raymond, K. N. *Chem. Soc. Rev.* **2007**, *36*, 161–171. Quan, M. L. C.; Cram, D. J. *J. Am. Chem. Soc.* **1991**, *113*, 2754–5.

(12) Marquez, C.; Hudgins, R. R.; Nau, W. M. *J. Am. Chem. Soc.* **2004**, *126*, 5806–5816.

(13) Lagona, J.; Fettingner, J. C.; Isaacs, L. *Org. Lett.* **2003**, *5*, 3745–3747. Wagner, B. D.; Boland, P. G.; Lagona, J.; Isaacs, L. *J. Phys. Chem. B* **2005**, *109*, 7686–7691.

(14) Lagona, J.; Fettingner, J. C.; Isaacs, L. *J. Org. Chem.* **2005**, *70*, 10381–10392.

(15) Huang, W.-H.; Liu, S.; Zavalij, P. Y.; Isaacs, L. *J. Am. Chem. Soc.* **2006**, *128*, 14744–14745. Huang, W.-H.; Zavalij, P. Y.; Isaacs, L. *Angew. Chem., Int. Ed.* **2007**, *46*, 7425–7427. Huang, W.-H.; Zavalij, P. Y.; Isaacs, L. *Org. Lett.* **2009**, *11*, 3918–3921.

(16) Huang, W.-H.; Zavalij, P. Y.; Isaacs, L. *J. Am. Chem. Soc.* **2008**, *130*, 8446–8454.

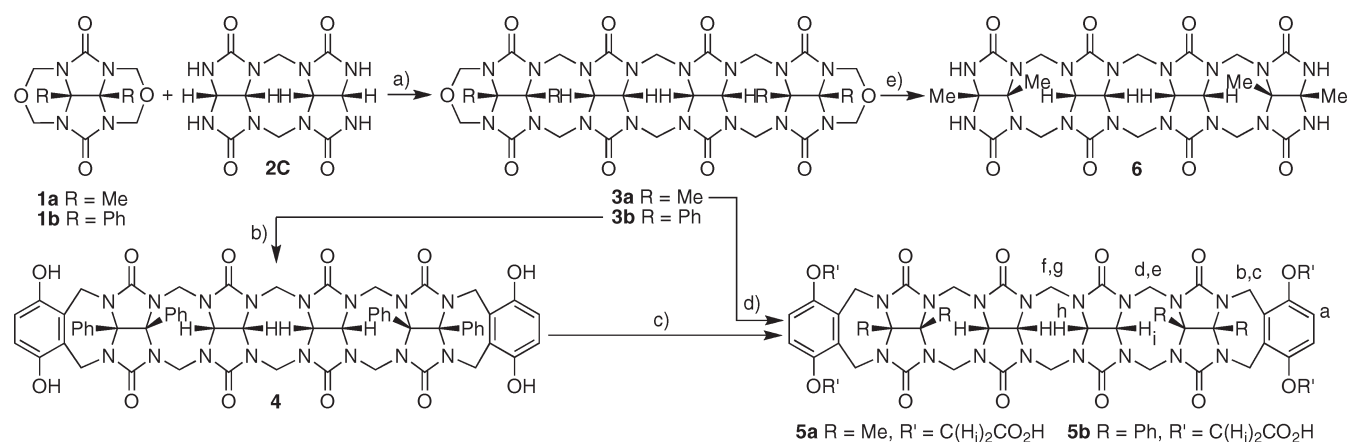
(17) Huang, W.-H.; Zavalij, P. Y.; Isaacs, L. *Org. Lett.* **2008**, *10*, 2577–2580.

(18) For reviews of the pioneering work of Nolte and Rebek on related systems, see: Rowan, A. E.; Elemans, J. A. A. W.; Nolte, R. J. M. *Acc. Chem. Res.* **1999**, *32*, 995–1006. Hof, F.; Craig, S. L.; Nuckolls, C.; Rebek, J., Jr. *Angew. Chem., Int. Ed.* **2002**, *41*, 1488–1508.

(19) Isaacs, L.; Witt, D. *Angew. Chem., Int. Ed.* **2002**, *41*, 1905–1907. Isaacs, L.; Witt, D.; Lagona, J. *Org. Lett.* **2001**, *3*, 3221–3224. Witt, D.; Lagona, J.; Damkaci, F.; Fettingner, J. C.; Isaacs, L. *Org. Lett.* **2000**, *2*, 755–758. Wu, A.; Chakraborty, A.; Fettingner, J. C.; Flowers, R. A., II; Isaacs, L. *Angew. Chem., Int. Ed.* **2002**, *41*, 4028–4031. Wu, A.; Isaacs, L. *J. Am. Chem. Soc.* **2003**, *125*, 4831–4835.

(20) Burnett, C. A.; Witt, D.; Fettingner, J. C.; Isaacs, L. *J. Org. Chem.* **2003**, *68*, 6184–6191.

(21) Stancl, M.; Hodan, M.; Sindelar, V. *Org. Lett.* **2009**, *11*, 4184–4187.

SCHEME 1. Synthesis of Acyclic CB[n] Congeners 5a and 5b and Tetramer 6^a

^aReagents and conditions: (a) MeSO₃H, 50 °C, (b) hydroquinone, TFA, reflux, (c) BrCH₂CO₂Et, K₂CO₃, CH₃CN, reflux then LiOH, MeOH/H₂O, 70 °C then concd HCl, (d) (EtO₂CCH₂O)₂C₆H₄, TFA, Ac₂O, reflux then LiOH, MeOH/H₂O, 70 °C then concd HCl, (e) 3,5-dimethylphenol, TFA, reflux.

lacks the substituted *o*-xylylene walls and study their recognition properties toward ammonium ions (7–32) in water.

Results and Discussion

This section is organized as follows. First, we describe the design and synthesis of acyclic CB[n] congeners 5a and 5b. Second, we discuss their conformational properties and X-ray crystal structures, and verify the absence of self-association of hosts 5a and 5b. Third, we use a combination of direct and competitive UV/vis spectroscopy and ¹H NMR spectroscopy to study the strength and geometrical details of the host–guest complexes of hosts 5a and 5b. Lastly, we discuss the trends in the tabulated values of *K*_a that give insights into the behavior of 5a and 5b.

Design and Synthesis of Acyclic CB[n] Congeners 5a and 5b. Hosts 5a and 5b are composed of a central methylene bridged glycoluril tetramer that is capped by two *o*-xylylene rings. The substituents (e.g., H and Ph or Me) on the central methylene bridged glycoluril tetramer all point away from the cavity, which preorganizes the oligomer into the C-shaped configuration required for binding. The bridging *o*-xylylene units are substituted with OCH₂CO₂H groups, which were expected to enable the synthetic route, enhance the solubility of 5a and 5b, and potentially enhance the binding affinity toward ammonium ions due to additional electrostatic (e.g., carboxylate·ammonium) interactions. The synthesis of the acyclic CB[n] congeners follows a building block approach (Scheme 1). First, glycoluril bis(cyclic ethers) 1a or 1b²² are reacted with C-shaped dimer 2C^{16,23} in MeSO₃H at 50 °C to yield tetramer bis(cyclic ethers) 3a (35%) and 3b (53%) in moderate yield. Compound 3a was reacted with hydroquinone in refluxing TFA to install the HO-substituted *o*-xylylene walls to yield 4. Compound 4 was then reacted with ethyl bromoacetate to yield an intermediate ester that was directly hydrolyzed to yield host 5b. For the synthesis of 5a we allowed 3a to react with (EtO₂CCH₂O)₂C₆H₄ under acidic conditions (TFA, Ac₂O) to yield an intermediate ester that was directly

hydrolyzed to yield 5a in moderate yield (32%). As a control compound to study the influence of the substituted *o*-xylylene walls we decided to prepare methylene bridged glycoluril tetramer 6. Heating 3a with 3,5-dimethylphenol as a formaldehyde scavenger¹⁴ in refluxing TFA delivered 6 in 45% yield.

Conformational Properties of 5a and 5b. The chemical structures of 5a and 5b greatly limit the conformational degrees of freedom of the system. For example, the fused bicyclic glycoluril ring system is conformationally locked. Similarly, the eight-membered rings that connect the glycolurils together by methylene bridges adopt the crown conformation that minimizes 1,5-diaxial interactions between substituents on the convex face of the glycoluril rings.²⁴ Finally, the seven-membered rings (7-MR) that connect the terminal substituted *o*-xylylene rings to the glycolurils have the potential to adopt two conformations (anti: *o*-xylylene ring oriented toward the cavity with 7-MR in chair conformation; syn: *o*-xylylene ring oriented away from the cavity with 7-MR in boat conformation). On the basis of previous studies by Nolte²⁵ and our group²⁰ we anticipated a preference for the anti conformation (vide infra, Figure 1a). In this manner, the 15 fused rings of 5a and 5b were designed to prefer a single conformation that preorganizes these acyclic hosts toward guest binding. Macrocyclization is not necessary.

X-ray Crystal Structures of Host 5b and Complexes 5b·20 and 5a·25. We were fortunate to obtain single crystals of 5b in its uncomplexed form (Figure 1a). As expected based on the precedent described above, 5b assumes a C-shaped conformation that defines a hydrophobic cavity. There are several interesting aspects of the structure of 5b that deserve comment. First, although the 15 fused rings effectively limit the conformation of the molecule to a C-shape, 5b is able to undergo out-of-plane twisting. Figure 1a shows that the substituted *o*-xylylene tips are skewed with respect to one another with one residing above the mean plane of the compound and the other below. This out-of-plane skewing results in an overall helical shape of 5b and therefore 5b

(22) Jansen, K.; Wego, A.; Buschmann, H.-J.; Schollmeyer, E.; Dopp, D. *Des. Monomers Polym.* **2003**, *6*, 43–55. Niele, F. G. M.; Nolte, R. J. M. *J. Am. Chem. Soc.* **1988**, *110*, 172–7.

(23) Zhao, Y.; Xue, S.; Zhu, Q.; Tao, Z.; Zhang, J.; Wei, Z.; Long, L.; Hu, M.; Xiao, H.; Day, A. I. *Chin. Sci. Bull.* **2004**, *49*, 1111–1116.

(24) Day, A. I.; Arnold, A. P.; Blanch, R. J. *Molecules* **2003**, *8*, 74–84. Ma, D.; Gargulakova, Z.; Zavalij, P. Y.; Sindelar, V.; Isaacs, L. *J. Org. Chem.* **2010**, *75*, 2934–2941.

(25) Sijbesma, R. P.; Kentgens, A. P. M.; Lutz, E. T. G.; van der Maas, J. H.; Nolte, R. J. M. *J. Am. Chem. Soc.* **1993**, *115*, 8999–9005. Sijbesma, R. P.; Wijnnga, S. S.; Nolte, R. J. M. *J. Am. Chem. Soc.* **1992**, *114*, 9807–13.

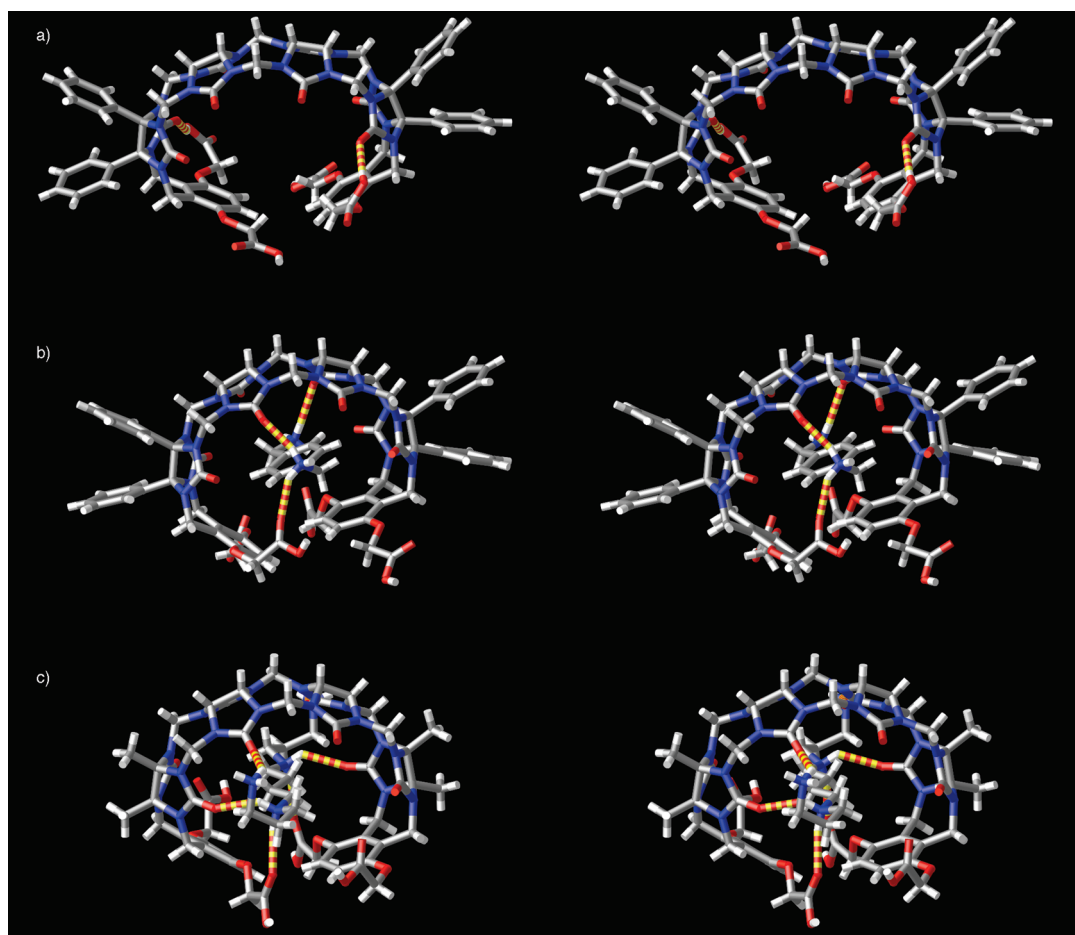


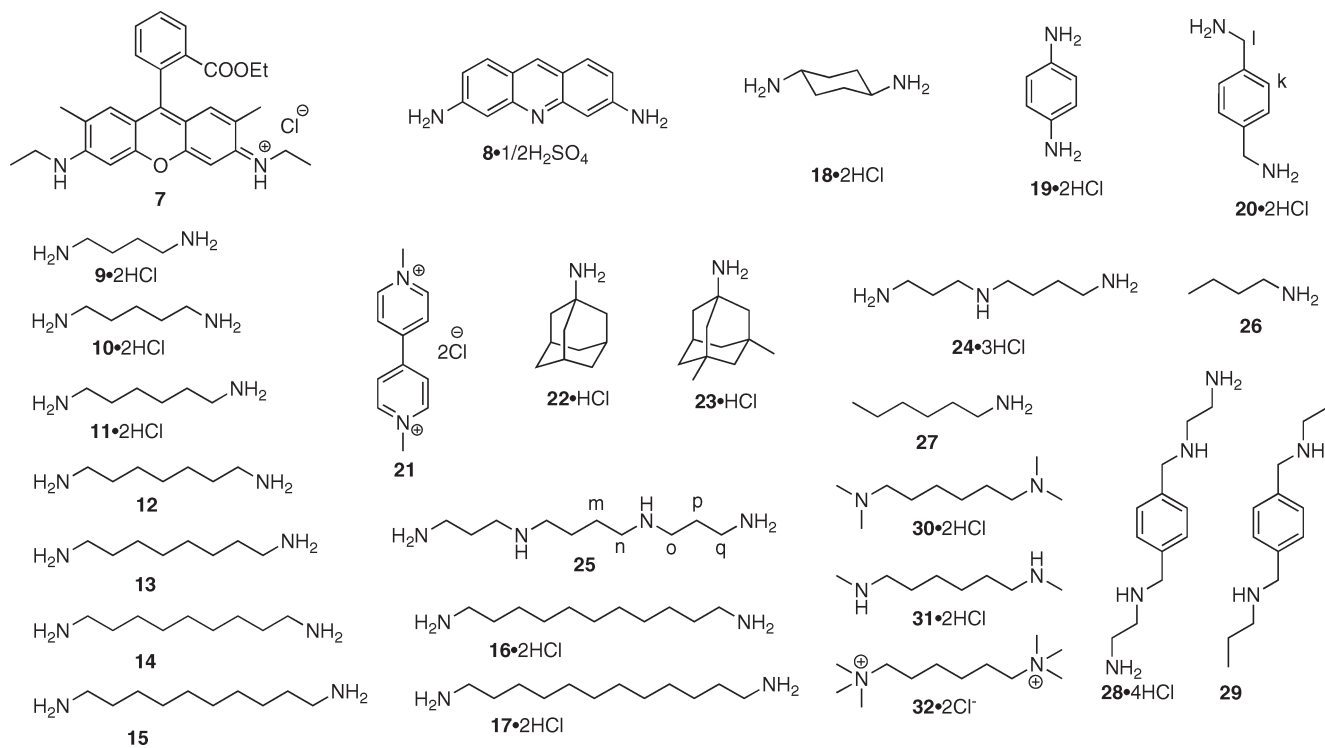
FIGURE 1. Cross-eyed stereoviews of the X-ray crystal structures of (a) **5b**, (b) **5b·20**, and (c) **5a·25**. Color code: C, gray; H, white; N, blue; O, red; H-bonds, red-yellow striped.

assumes a chiral conformation in the crystal. Within the crystal of **5b** there are equal amounts of the two enantiomeric forms of **5b**. Second, the $\text{OCH}_2\text{CO}_2\text{H}$ groups on the *o*-xylylene rings are oriented roughly parallel to the cavity. In the neutral form of **5b** present in the crystal, the CO_2H groups form intramolecular H-bonds back to the ureidyl $\text{C}=\text{O}$ portal of **5b** as expected on the basis of its highly negative electrostatic potential. Third, although the chemical structure of **5b** contains six units (e.g., four glycolurils and two *o*-xylylene rings) the cavity of **5b** appears to be larger than that of $\text{CB}[6]$. To quantify this effect we consider the distance between the quaternary (PhC) carbon atoms on opposite sides of **5b** and $\text{CB}[n]$. The relevant distances for **5b** are 11.91 and 12.60 Å. Comparable values for $\text{CB}[5]$ are 8.48 and 7.60 Å, for $\text{CB}[6]$ are 10.05 and 10.05 Å, for $\text{CB}[7]$ are 10.74 and 11.37 Å, and for $\text{CB}[8]$ are 11.47 and 12.54 Å. By this measure, the curvature of the methylene bridged glycoluril tetramer subunit of **5b** is most similar to that of $\text{CB}[8]$. However, the 7-MR adopt a chairlike conformation that projects the connected substituted *o*-xylylene rings into the cavity of **5b** at a sharper angle than is observed for $\text{CB}[6]$ – $\text{CB}[8]$. In this manner it appears that **5b** contains structural regions that resembles $\text{CB}[8]$ and other regions that are similar to smaller $\text{CB}[n]$.

Figure 1b shows a stereoview of the X-ray crystal structure of **5b·20**. In this structure, **20** is bound within the cavity of **5b**

and is held in place by two ureidyl $\text{C}=\text{O}\cdots\text{HN}$ H-bonds and one carboxylic acid $\text{C}=\text{O}\cdots\text{HN}$ H-bond. Host **5b** undergoes a structural change that decreases the size of the host cavity in the **5b·20** complex. This structural change is reflected in the decreased distance between the opposing quaternary PhC carbon atoms (11.44 and 11.85 Å). In addition, one of the terminal *o*-xylylene rings of **5b** engages in an offset π – π stacking interaction (mean plane separation = 3.45 Å; centroid–centroid distance = 3.74 Å) with the aromatic ring of guest **20**. Figure 1c shows a stereoview of the X-ray crystal structure of **5a·25**. Spermine **25** is bound within the cavity of **5a** by virtue of four H-bonds between the central $-\text{NH}_2^+$ groups of **25** and the ureidyl $\text{C}=\text{O}$ groups and the carboxylic acid groups of **25**. In addition, each of the terminal $-\text{H}_2\text{N}^+(\text{CH}_2)_3\text{NH}_3^+$ groups folds back and form additional H-bonds to the $\text{C}=\text{O}$ portal of **5a**. In total the **5a·25** complex benefits from six H-bonds. One of the interesting structural features of the **5a·25** complex is the pronounced out-of-plane skewing of the terminal *o*-xylylene rings. This geometrical feature places the CH_2 groups of the central butylene linker within the shielding region of the adjacent aromatic ring, which is reflected in the large upfield shifts observed for H_m and H_n in the ^1H NMR spectrum of the **5a·25** complex (vide infra). Overall, hosts **5a** and **5b** exhibit a substantial ability to respond to the structural characteristics of the guest.

CHART 2. Chemical Structures of Guests Used in This Study



Hosts 5a, 5b, and 6 Do Not Undergo Self-Association. In our previous studies of methylene bridged glycoluril oligomers bearing terminal *o*-xylylene walls self-association has been an important and in some cases dominant mode of interaction.¹⁹ Therefore, before proceeding to study the host–guest recognition properties of **5a**, **5b**, and **6** we wanted to rule out the possibility of self-association in water. For this purpose we performed ¹H NMR dilution experiments (Supporting Information) and do not observe any changes in chemical shift over the 60 μM to 1.52 mM range of concentration. These results indicate that **5a**, **5b**, and **6** do not undergo self-association, which allows us to study their host–guest recognition properties free of these effects.

Binding Studies between Hosts 5a, 5b, and 6 and Guests 7–32. This section describes the noncovalent interaction between the hosts and guests 7–32 (Chart 2) by several different methods.

¹H NMR Investigations of the Binding Interactions. Initially, we used ¹H NMR to study the interaction between **5b** and **20**. Figure 2a–c shows the ¹H NMR spectra recorded for **5b**, **20**, and for an equimolar mixture of **5b** and **20**. The protons on the aromatic ring of **20** undergo a substantial upfield shift in the presence of **5b** suggesting that **20** is bound within the cavity of **5b**, which is corroborated by the X-ray crystal structure of **5b**·**20** (Figure 1b). When **5b** and **20** are mixed at a 1:2 stoichiometry we observe resonances for free **20** and complexed **20**, which establishes that the dynamics of exchange are slow on the chemical shift time scale. Attempts to perform ¹H NMR titration experiments to determine values of K_a were unsuccessful because they exceeded those that can be determined accurately ($K_a < 10^5 \text{ M}^{-1}$) by this technique.²⁶

Figure 2d–f shows the ¹H NMR recorded for **5a**, spermine **25**, and an equimolar mixture of **5a** and **25**. In this case the pattern of upfield shift of the resonances for guest **25** suggests that the central diaminobutane linker of **25** is bound within the central cavity of **5a** with the $\text{N}(\text{CH}_2)_3\text{NH}_3^+$ arms extending past the ureidyl C=O portals of **5a**. This interpretation is supported by the X-ray crystal structure of the **5a**·**25** shown in Figure 1c and discussed below.

Direct UV/Vis Titrations. Because the values of K_a for the interaction between **5a** and **20** were inaccessible by ¹H NMR titrations we decided to resort to competitive UV/vis binding assays. We used competitive UV/vis binding assays rather than the competitive ¹H NMR binding method used by us previously⁶ because most of the complexes of **5a** display fast exchange kinetics on the chemical shift time scale. We found that dye **7** (rhodamine 6G) binds to **5a** and undergoes changes in its UV/vis spectrum. Figure 3a shows the UV/vis spectra recorded when a fixed concentration of **7** (9.23 μM) was titrated with **5a** (0–49 μM). The UV/vis spectra show large changes at 520 and 550 nm and the presence of an isosbestic point at 533 nm that allowed us to conclude that **5a** and **7** undergo clean formation of the **5a**·**7** complex. Figure 3b shows a plot of UV/vis absorbance at 520 nm versus the concentration of **5a** that can be fitted to a 1:1 binding model to determine the stability of the **5a**·**7** complex ($K_a = (2.1 \pm 0.1) \times 10^5 \text{ M}^{-1}$). With this value of K_a in hand it is possible to measure K_a values for weaker binding guests by competitive indicator displacement assays.²⁷

UV/vis Indicator Displacement Assays. In indicator displacement assays, a complex is formed between a host and an indicator that undergoes a UV/vis change upon complexation. Upon addition of a competitive binding guest, the

(26) Connors, K. A. *Binding Constants*; John Wiley & Sons: New York, 1987.

(27) Wiskur, S. L.; Ait-Haddou, H.; Lavigne, J. J.; Anslyn, E. V. *Acc. Chem. Res.* **2001**, *34*, 963–972. Anslyn, E. V. *J. Org. Chem.* **2007**, *72*, 687–699.

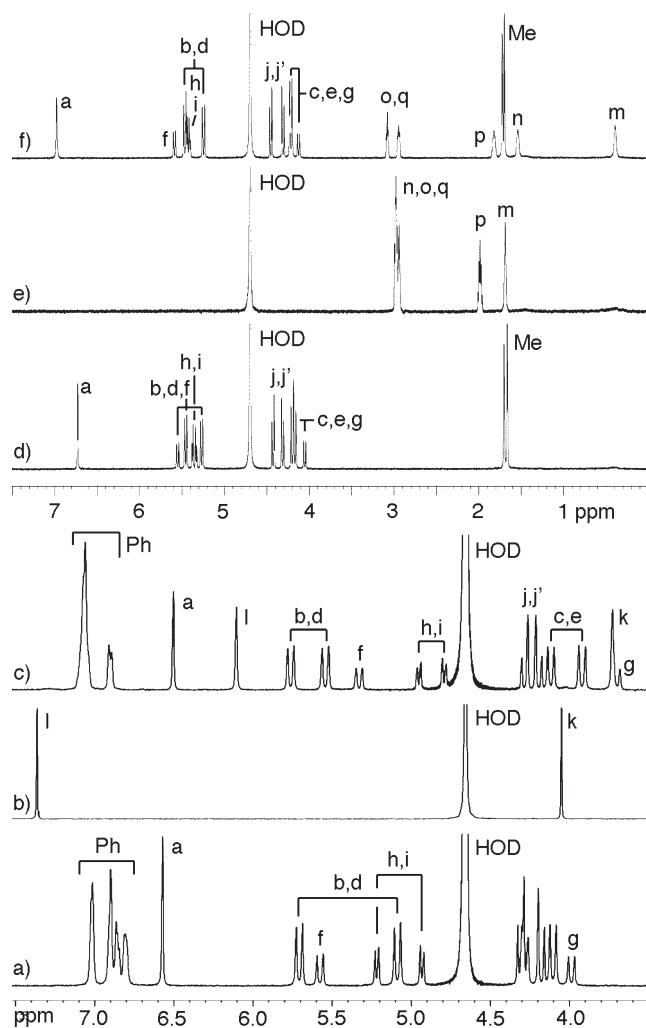


FIGURE 2. ^1H NMR spectra recorded for (a) **5b**, (b) **20**, and (c) an equimolar mixture of **5b** and **20** (400 MHz, room temperature, 25 mM sodium phosphate buffered D_2O , pH 7.4) and (d) **5b**, (e) **25**, and (f) an equimolar mixture of **5b** and **25** (600 MHz, room temperature, 25 mM sodium phosphate buffered D_2O , pH 7.4).

indicator is released resulting in a UV/vis spectral change. On the basis of a knowledge of the concentrations employed and the value of K_a for either the host·indicator complex or the host·guest interaction it is possible to calculate the unknown K_a . We used this strategy (Supporting Information) with dyes (indicators) **7** and **8** to determine the values of K_a for the complexes between host **5a** and guests **9–30** (Table 1). We first used the competition between UV/vis inactive guest butylammonium ion **26** and rhodamine G (**7**) to determine the stability of the **5a**·**26** complex ($K_a = (1.4 \pm 0.1) \times 10^5 \text{ M}^{-1}$). Subsequently we performed an indicator displacement assay between **5a**, UV/vis active acridine dye **8**, and **26** that allowed us to determine the value of K_a for the **5a**·**8** complex ($K_a = (7.2 \pm 0.4) \times 10^8 \text{ M}^{-1}$). We then measured the values of K_a for the remaining complexes of **5a** by indicator displacement assays using the **5a**·**8** complex (Table 1). The data from the UV/vis competition assays and their analysis to extract the K_a values are given in the Supporting Information. Table 1 also presents the literature

(28) Rekharsky, M. V.; Ko, Y.-H.; Selvapalam, N.; Kim, K.; Inoue, Y. *Supramol. Chem.* **2007**, *19*, 39–46.

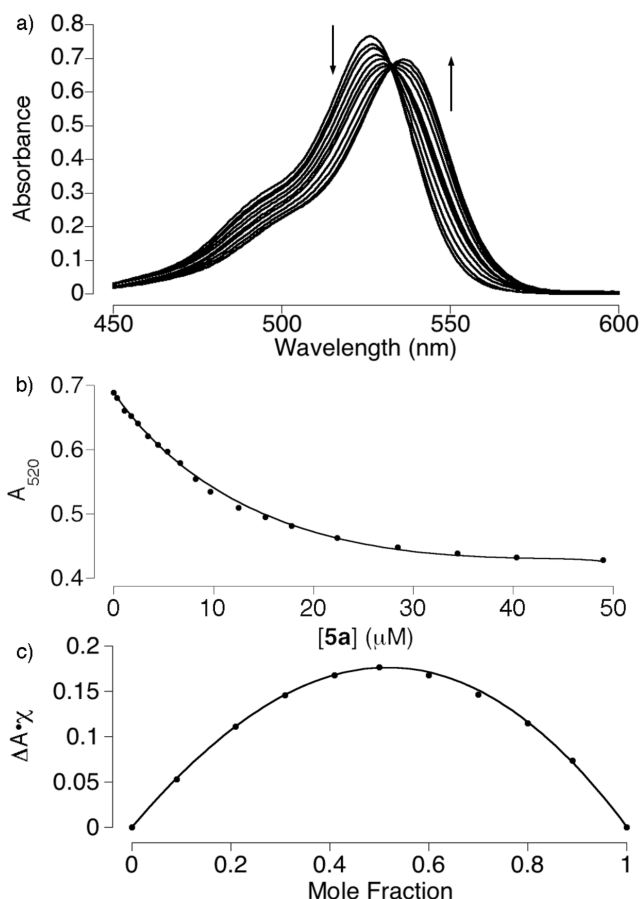


FIGURE 3. (a) UV/vis spectra obtained during the titration of a fixed concentration of **7** ($9.23 \mu\text{M}$) with **5a** ($0\text{--}49 \mu\text{M}$); (b) plot of absorbance versus $[\text{7}]$ used to determine the value of K_a by nonlinear least-squares fitting; and (c) Job plot ($[\text{5a}] + [\text{7}] = 7.65 \mu\text{M}$) of mole fraction of **5a** versus $\Delta A \times \chi$.

values of the binding constants for a subset of these guests toward $\text{CB}[6]$ ^{5,28} and $\text{CB}[7]$.^{6,29}

Trends in the Values of K_a between Host **5a and Guests.** The values of K_a given in Table 1 derived from the work of Mock,⁵ Isaacs,⁶ and Inoue²⁸ allow us to make comparisons between various guests that shed light on the overall binding properties of **5a** compared to $\text{CB}[n]$.

Influence of Chain Length. One of the best studied phenomena in the binding properties of the $\text{CB}[n]$ family is the influence of guest length on the binding affinity of alkanediammonium ions. For the relatively rigid host $\text{CB}[6]$ a maximum binding affinity is seen for pentanediammonium and hexanediammonium ions **10** and **11** with greatly reduced affinity toward longer and shorter diammonium ions.^{5,28} Figure 4 shows a plot of binding affinity of **5a** and $\text{CB}[6]$ toward diammonium ions **9–17** as a function of chain length in the competitive medium 1:1 $\text{H}_2\text{O}:\text{HCO}_2\text{H}$ determined by Mock⁵ and in the less competitive medium 50 mM NaCl determined by Inoue.²⁸ Several trends in these data are worth noting. First, host **5a** binds more tightly to the longer

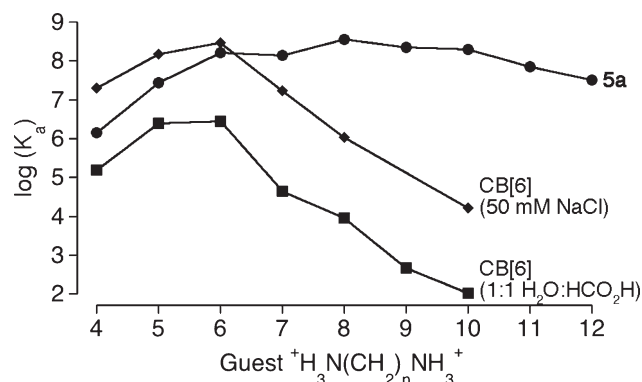
(29) Values of K_a for some of the other guests are available from the literature, but were measured with different buffers or pH values. To avoid additional complications due to these effects we have restricted our discussion to values of K_a from the systematic works of Mock, Inoue, and our group.

TABLE 1. Binding Constants (K_a) for the Interaction of Hosts **5a, CB[6], and CB[7] with Various Guests**

guests	K_a (M^{-1})		
	host 5a	CB[6]	CB[7] ^b
7	$(2.1 \pm 0.1) \times 10^5$		
8	$(7.2 \pm 0.4) \times 10^8$		
9	$(1.4 \pm 0.1) \times 10^6$	1.5×10^5 ^a	
10	$(2.8 \pm 0.3) \times 10^7$	$(2.0 \pm 0.2) \times 10^7$ ^c	
11	$(1.6 \pm 0.1) \times 10^8$	$(1.5 \pm 0.1) \times 10^8$ ^c	$(9.0 \pm 1.4) \times 10^7$
12	$(1.4 \pm 0.1) \times 10^8$	$(2.8 \pm 0.6) \times 10^8$ ^b	
13	$(3.6 \pm 0.4) \times 10^8$	$(2.9 \pm 0.2) \times 10^8$ ^c	
14	$(2.2 \pm 0.2) \times 10^8$	4.3×10^4 ^a	
15	$(2.0 \pm 0.2) \times 10^8$	$(1.7 \pm 0.2) \times 10^7$ ^c	
16	$(7.2 \pm 0.7) \times 10^7$	9.1×10^3 ^a	
17	$(3.2 \pm 0.3) \times 10^7$	$(1.08 \pm 0.06) \times 10^6$ ^c	
18	$(4.3 \pm 0.4) \times 10^7$	4.8×10^2 ^a	$(2.3 \pm 0.4) \times 10^7$
19	$(7.1 \pm 0.8) \times 10^5$	1.0×10^2 ^a	$(2.1 \pm 0.3) \times 10^6$
20	$(6.8 \pm 0.9) \times 10^8$	$(3.1 \pm 0.2) \times 10^6$ ^c	$(1.8 \pm 0.3) \times 10^9$
21	$(4.0 \pm 0.4) \times 10^8$	2.2×10^3 ^a	$(1.3 \pm 0.2) \times 10^7$
22	$(3.5 \pm 0.4) \times 10^6$	$(1.67 \pm 0.08) \times 10^5$ ^c	$(4.2 \pm 1.0) \times 10^{11}$
23	$(4.8 \pm 0.5) \times 10^5$		$(2.5 \pm 0.4) \times 10^4$
24	$(2.6 \pm 0.4) \times 10^7$	1.4×10^6 ^a	
25	$(4.5 \pm 0.4) \times 10^8$	$(4.1 \pm 0.3) \times 10^8$ ^c	
26	$(1.4 \pm 0.1) \times 10^5$	1.3×10^7 ^a	
27	$(1.4 \pm 0.1) \times 10^6$	$(3.3 \pm 0.4) \times 10^9$ ^c	
28	$(3.6 \pm 0.5) \times 10^9$	1.0×10^5 ^a	
29	$(2.0 \pm 0.2) \times 10^9$	$(3.1 \pm 0.2) \times 10^6$ ^c	
30	$(9.8 \pm 0.9) \times 10^7$	2.2×10^3 ^a	
31	$(3.1 \pm 0.4) \times 10^8$	$(1.67 \pm 0.08) \times 10^5$ ^c	
32	$(1.4 \pm 0.2) \times 10^8$		

^aMeasured in H₂O/85% HCO₂H (1:1).⁵ ^bMeasured in 50 mM NaOAc buffer, pH 4.74. ^cMeasured in 50 mM NaCl.²⁸

alkanediammonium ions (**12–15**) than CB[6] does. These higher binding constants may reflect (1) that the larger hydrophobic cavity of **5a** (relative to CB[6]) provides a larger hydrophobic driving force toward complexation and/or (2) the energetic contributions of the interaction between the CO₂⁻ arms of host **5a** and the diammonium guest (vide infra). Second, host **5a** appears to be less sensitive to changes in length than CB[6]; host **5a** is less selective than CB[6] and binds **11–15** with high affinity ($K_a > 10^8 M^{-1}$). We believe this lower selectivity is due to the structural flexibility of host **5a** relative to CB[6]. For example, when host **5a** adopts a skewed (helical) conformation the distance between its ureidyl C=O portals also change. It is well-known that the ureidyl C=O portals of CB[*n*] provide a significant portion of the driving force for the binding of ammonium ions by ion-dipole/H-bonding interactions. Because host **5a** is acyclic it may increase its cavity size by flexing its pairs of CH₂ bridges. This process allows **5a** to accommodate longer guests perhaps by folding the hydrophobic chain of the guest inside the host.^{17,30} Indeed the ¹H NMR spectra of the complexes between **5a** and **13**, **15**, and **17** (Supporting Information)

**FIGURE 4.** Plot of $\log(K_a)$ versus chain length for the interaction between alkanediammonium ions (**9–17**) and hosts **5a** (●), CB[6] in 1:1 H₂O:HCO₂H (■), and CB[6] in 50 mM NaCl (◆).

show significant upfield shifts for all of the CH₂ groups indicating that they are within the hydrophobic cavity of **5a** rather than outside the cavity or near the C=O portals.

Binding Capacity of 5a. On the basis of the analysis of the X-ray structure of **5a** (Figure 1) and the ability of **5a** to bind the longer diammonium ions tightly (e.g., decanediammonium ion **15**) we anticipated that host **5a** would be able to complex larger guests that typically only bind to the more spacious hosts CB[7] and CB[8]. For this purpose, we studied the binding affinity of **5a** toward guests **18–23** that display a range of guest sizes. For example, CB[6] binds to the smaller guests **19** and **20**, CB[7] can accommodate slightly larger guests **18**, **21**, and **22**, and CB[8] is able to bind tightly even to dimethyl adamantaneammonium ion **23**.⁶ In contrast, host **5a** forms complexes with all six size probe guests **18–23** albeit with differences in affinity. For example, host **5a** binds relatively weakly to the smallest (**19**, $K_a = 7.1 \times 10^5 M^{-1}$) and largest (**23**, $K_a = 4.8 \times 10^5 M^{-1}$) guests in this series. The intermediate sized guests **18**, **20**, and **21** are all bound more tightly by **5a**. These higher levels of affinity may be due to a better size match between the cavity of host **5a** and guests **18**, **20**, and **21**, the possibility of π - π interactions between guests **20** or **21** and the substituted *o*-xylylene walls of host **5a**, or a combination of these factors. The ¹H NMR spectra recorded for the **5a**·**18**, **5a**·**21**, and **5a**·**22** complexes (Supporting Information) show upfield shifts for all of the guest protons indicating that the guests reside inside the anisotropic shielding region defined by the aromatic rings and glycoluril tetramer subunits of **5a**. In combination these results suggest that the effective cavity volume of **5a** is similar to or slightly larger than that of CB[7] ($V = 272 \text{ \AA}^3$).³ It is worth noting that the affinity of **5a** toward several of these size probe guests (**18**, **21**, and **23**) exceeds the K_a values measured toward CB[7] (Table 1). In contrast, the affinity of CB[7] toward its best guests (**20** and **22**) is greater than that measured toward **5a**. These results reinforce our belief that the flexibility of **5a** makes it a more general purpose high affinity but modest selectivity host in water.

Effect of the Number of Ammonium Groups. In his pioneering work Mock demonstrated that the addition of ammonium groups to guests for CB[6] generally resulted in a 10–1000-fold increase in binding affinity.^{5,28} This effect is also seen for other CB[*n*]. For example, spermine **25** ($K_a = 1.3 \times 10^7 M^{-1}$) binds ca. 10-fold stronger to CB[6] than

(30) Ko, Y. H.; Kim, H.; Kim, Y.; Kim, K. *Angew. Chem., Int. Ed.* **2008**, *47*, 4106–4109.

spermidine **24** ($K_a = 1.4 \times 10^6 \text{ M}^{-1}$), that in turn binds ca. 10-fold stronger to CB[6] than butanediammonium ion (**9**, $K_a = 1.5 \times 10^5 \text{ M}^{-1}$) does. The values of K_a contained in Table 1 allow us to ascertain whether similar trends hold for **5a**. For example, butylammonium ion (**26**, $K_a = 1.4 \times 10^5 \text{ M}^{-1}$) binds 10-fold weaker to **5a** than butanediammonium ion (**9**, $K_a = 1.4 \times 10^6 \text{ M}^{-1}$) does. Similarly, hexylammonium ion (**27**, $K_a = 1.4 \times 10^6 \text{ M}^{-1}$) binds ca. 100-fold weaker to **5a** than hexanediammonium ion (**11**, $K_a = 1.6 \times 10^8 \text{ M}^{-1}$). Related trends (17–185-fold increase in K_a per ammonium group) can be seen when comparing the binding of butanediammonium ion (**9**, $K_a = 1.4 \times 10^5 \text{ M}^{-1}$) with that of triammonium ion spermidine **24** ($K_a = 2.6 \times 10^7 \text{ M}^{-1}$) and tetraammonium ion spermine **25** ($K_a = 4.5 \times 10^8 \text{ M}^{-1}$). Acyclic CB[*n*] congener **5a** displays similar gains in K_a as a result of additional ammonium groups as CB[6] does.

Effect of the Degree of Alkylation of the Ammonium Ion. The affinity of CB[6] toward alkanediammonium ions is dramatically affected by the degree of alkylation of the N-atoms. For example, CB[6] binds tightly to hexanediammonium ion **11** ($K_a = 2.8 \times 10^6 \text{ M}^{-1}$) and *N,N'*-dimethylhexanediammonium ion **31** ($K_a = 1.7 \times 10^6 \text{ M}^{-1}$) but binds only weakly to *N,N,N',N'*-tetramethylhexanediammonium ion **30** ($K_a = 9.1 \times 10^3 \text{ M}^{-1}$). This effect can be explained based on the geometry of the CB[6]·**11** complex (Chart 1) that possesses two N–H···O=C H-bonds per portal. Accordingly, each ammonium ion can have two C-substituents and 2 H-atoms and still assume this ideal geometry; addition of a third C-substituent (e.g., **30**) results in severe steric interactions between host and guest. The affinity of **5a** toward **11** ($K_a = 1.8 \times 10^8 \text{ M}^{-1}$), **31** ($K_a = 3.1 \times 10^8 \text{ M}^{-1}$), **30** ($K_a = 9.8 \times 10^7 \text{ M}^{-1}$), and **32** ($K_a = 1.4 \times 10^8 \text{ M}^{-1}$) does not follow a similar trend. The comparable affinities of **5a** toward **11**, **31**, **30**, and **32** suggest that the flexibility of **5a** allows it to compensate for the loss of N–H···O=C H-bonds by adjusting the size of the cavity to best accommodate the geometrical requirements of the interaction between the ammonium ion and the ureidyl C=O portal. The ¹H NMR spectra recorded for **5a**·**11**, **5a**·**30**, **5a**·**31**, and **5a**·**32** show remarkably similar patterns of upfield shifts of the central CH₂ groups and very little change in chemical shift for the NMe groups (Supporting Information). This suggests that all four complexes (**5a**·**11**, **5a**·**30**, **5a**·**31**, and **5a**·**32**) possess a similar overall geometry with the hexylene chain fully bound inside the cavity of **5a**.

Effect of the Concentration of Buffer Used. It is well-known from CB[*n*] supramolecular chemistry that the presence of metal cations in solution reduces their apparent binding affinity toward guests due to competitive binding at the electrostatically negative ureidyl C=O lined portals.^{12,20,31} We hypothesized that the ureidyl C=O portals of acyclic CB[*n*] congeners **5a** and **5b** that are shaped by four contiguous glycoluril units should also bind to metal cations and thereby reduce their affinity toward guests. Accordingly, we measured the affinity of rhodamine 6G (**7**) toward **5b** by direct UV/vis titration in sodium phosphate buffer (pH 7.4) at different concentrations. Figure 5 shows a plot of K_a versus phosphate concentration. As the concentration of sodium phosphate is increased the log K_a value undergoes a steady decrease as expected based on competitive binding

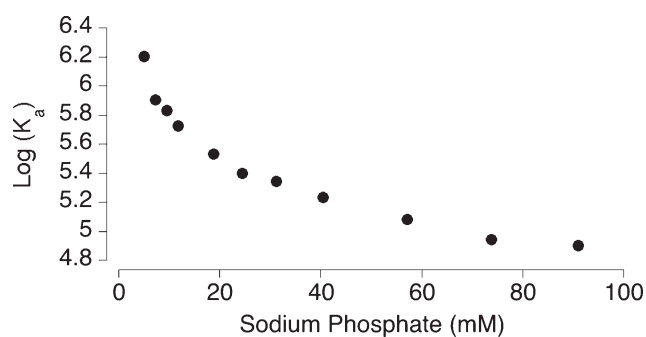


FIGURE 5. Plot of log K_a versus the concentration of sodium phosphate buffer (H_2O , pH 7.4) for the formation of the **5b**·**7** complex.

of Na^+ for the C=O portals of **5b**. This analysis indicates that the ureidyl C=O portals of host **5b** retain this essential feature of the CB[*n*] family that supports our description of **5a** and **5b** as acyclic CB[*n*] congeners.

Contribution of the Substituted *o*-Xylylene Walls to the Binding. On the basis of the excellent binding affinity of **5a** toward the aromatic guests **8**, **20**, **21**, **28**, and **29** and the X-ray structure of **5b**·**20** (Figure 1b) we suspected that π – π interactions between the substituted *o*-xylylene walls of **5a** and the aromatic rings of the guest might be an important driving force in the recognition behavior of host **5a**. Accordingly, we prepared compound **6** that lacks the substituted *o*-xylylene walls of **5a**. We measured the value of K_a for the interaction between **6** and hexanediammonium ion (**11**, $K_a = (5.6 \pm 0.4) \times 10^3 \text{ M}^{-1}$) or *p*-xylenediammonium ion (**20**, $K_a = (1.5 \pm 0.1) \times 10^4 \text{ M}^{-1}$) by direct ¹H NMR titrations (Supporting Information). These K_a values are substantially smaller than the corresponding values for the interaction of **5a** with **11** ($K_a = (1.6 \pm 0.1) \times 10^8 \text{ M}^{-1}$) and **20** ($K_a = (6.8 \pm 0.9) \times 10^8 \text{ M}^{-1}$). This indicates that the substituted *o*-xylylene walls of **5a** do contribute substantially to the overall binding behavior of **5a**. The fact that reduction in affinity for aliphatic **11** ((2.8×10^4) -fold) is comparable to that of aromatic **20** ((4.5×10^4) -fold) suggests that the aromatic walls do not engage in strong specific π – π interactions but instead probably enhance binding by defining a structured environment that releases water upon binding. To ascertain the potential contributions of carboxylate–ammonium ion electrostatic interactions on the recognition behavior of **5a** we compared its binding toward **28** and **29**. Both **28** and **29** are derivatives of *p*-xylenediamine; **29** contains two $\text{CH}_2\text{CH}_2\text{CH}_3$ arms whereas **28** contains two $\text{CH}_2\text{CH}_2\text{NH}_3^+$ arms. We specifically chose the two carbon linkers to prevent backfolding of the $\text{CH}_2\text{CH}_2\text{NH}_3^+$ arms to the ureidyl C=O portals of **5a** and potentially promote carboxylate–ammonium ion electrostatic interactions in the **5a**·**28** complex. Experimentally, we find that the binding constants measured for **5a**·**28** and **5a**·**29** are quite similar, which suggests that carboxylate–ammonium ion electrostatic interactions do not play a large role in the recognition behavior of **5a**.

Conclusions

In summary, we have presented the synthesis of acyclic CB[*n*] congeners **5a** and **5b** that contain four contiguous methylene bridged glycoluril units. Despite the acyclic nature of **5a** and **5b** the 15 fused rings effectively preorganize **5a** and **5b** into a C-shape required for binding. By a combination of direct UV/vis titrations along with indicator displacement

(31) Buschmann, H. J.; Cleve, E.; Schollmeyer, E. *Inorg. Chim. Acta* **1992**, *193*, 93–97. Jeon, Y.-M.; Kim, J.; Whang, D.; Kim, K. *J. Am. Chem. Soc.* **1996**, *118*, 9790–9791. Ong, W.; Kaifer, A. E. *J. Org. Chem.* **2004**, *69*, 1383–1385.

assays we determined the values of K_a for the interaction of **5a** with a variety of guest compounds (7–32). We find that **5a** acts as a high affinity host—just like CB[n]—with binding constants in the 10^5 – 10^9 M⁻¹ range. The cavity volume of host **5a** is comparable to that of CB[7]. Unlike CB[n], **5a** displays only moderate levels of selectivity based on guest length and the degree of alkylation of the N-atoms of the ammonium ion guests. We attribute this lower selectivity to the conformational changes of the host that occur upon formation of the host-guest complexes. Similar to CB[n], the binding affinity of **5a** toward its guests increases by a factor of 10–1000 as the number of ammonium ions in the guests is increased (e.g., **9** vs **24** vs **25**) whereas the affinity is reduced as the concentration of metal cations in the buffer increases due to competitive binding at the ureidyl C=O portals.

To date, three major issues for the use of CB[n] compounds in practical applications have been the following: (1) their generally poor solubility in aqueous solution, (2) challenges for their selective functionalization, and (3) the relatively slow uptake and release rates of guests due to the constrictive binding nature of the CB[n] cavity. The acyclic CB[n] congeners presented in this paper were prepared by convergent building block routes and feature terminal *o*-xylylene rings that are readily functionalized and endowed with carboxylic acid groups that increase solubility in aqueous solution. By virtue of its fused ring acyclic structure **5a** is both preorganized for ammonium ion binding and capable of fast uptake and release of its guests. Macrocyclization is not necessary to achieve high affinity interactions between acyclic CB[n] congeners and ammonium ion guests. The availability of acyclic CB[n] congeners that can be readily functionalized while maintaining the outstanding recognition properties of the CB[n] family promises their future use in a variety of applications including chemical sensing, controlled release or sequestration, and as a component of molecular machines.

Experimental Section

General Experimental. Starting materials were purchased from commercial suppliers and were used without further purification. Compounds **1a**, **1b**, **2C**, **28**, and **29** were prepared according to literature procedures.^{16,22,32} Melting points were measured in open capillary tubes and are uncorrected. TLC analysis was performed with use of precoated plastic plates. IR spectra were recorded on a FT-IR spectrometer (reported in cm⁻¹). NMR spectra were measured on spectrometers operating at 400 MHz for ¹H and 100 MHz for ¹³C. Mass spectrometry was performed with the electrospray ionization (ESI) technique.

Compound 3a: To a mixture of **2C** (7.42 g, 24.0 mmol) in anhydrous MeSO₃H (55 mL) was added **1a** (24.46 g, 96.2 mmol). The mixture was stirred and heated at 50 °C for 3 h. The reaction mixture was poured into water (700 mL). After filtration, the crude solid was dried in high vacuum. The crude solid was recrystallized from TFA (15 mL) and water (45 mL) to yield **3a** as a white solid (6.60 g, 8.45 mmol, 35%). Mp > 227 °C dec. IR (ATR, cm⁻¹): 1714 s, 1456 m, 1314 m, 1223 s, 1177 s, 1079 m, 960 m, 920 m, 857 m, 799 s, 757 m, 668 m. ¹H NMR (400 MHz, DMSO-*d*₆): δ 5.65 (d, *J* = 14.6 Hz, 2H), 5.50 (d, *J* = 15.2 Hz,

4H), 5.48 (d, *J* = 8.6 Hz, 2H), 5.34 (d, *J* = 8.6 Hz, 2H), 5.12 (d, *J* = 10.9 Hz, 4H), 4.79 (d, *J* = 10.9 Hz, 4H), 4.18 (d, *J* = 15.2 Hz, 4H), 4.14 (d, *J* = 14.6 Hz, 2H), 1.76 (s, 6H), 1.59 (s, 6H). ¹³C NMR (100 MHz, TFA, DMSO-*d*₆ as internal reference): δ 157.0, 156.6, 78.5, 74.5, 71.2, 71.0, 70.6, 52.3, 48.1, 15.5, 14.4. MS (ESI): *m/z* 781 ([M + H]⁺).

Compound 3b: A mixture of **2C** (0.920 g, 3.00 mmol) and **1b** (2.61 g, 6.90 mmol) in MeSO₃H (10 mL) was stirred at room temperature for 20 min. Then the mixture was stirred and heated at 50 °C for 4 h. The reaction mixture was poured into MeOH (500 mL). After filtration, the crude solid was dried in high vacuum. The crude solid was recrystallized from TFA (25 mL) and water (25 mL) to yield **3b** as a white solid (1.700 g, 1.65 mmol, 53%). Mp > 350 °C. TLC (MeCN/H₂O, 4:1) *R*_f 0.47. IR (cm⁻¹): 3450 w, 1722 s, 1445 m, 1362 m, 1314 m, 1198 s. ¹H NMR (400 MHz, DMSO-*d*₆): δ 7.13–6.94 (m, 20H), 5.82 (d, *J* = 15.2 Hz, 4H), 5.68 (d, *J* = 14.8 Hz, 2H), 5.38 (d, *J* = 10.4 Hz, 4H), 5.20 (d, *J* = 9.2 Hz, 2H), 5.03 (d, *J* = 9.2 Hz, 2H), 4.32 (d, *J* = 10.4 Hz, 4H), 4.08 (d, *J* = 14.8 Hz, 2H), 4.05 (d, *J* = 15.2 Hz, 4H). ¹³C NMR (100 MHz, TFA, DMSO-*d*₆ as internal reference): δ 159.6, 157.5, 130.7, 130.3, 129.6, 128.9, 128.3, 128.2, 127.4, 87.8, 81.9, 72.3, 72.0, 71.6, 53.2, 50.6. MS (ESI): *m/z* 1029 ([M + H]⁺).

Compound 5a: To a mixture of **3a** (6.56 g, 8.36 mmol) and **4** (17.9 g, 66.9 mmol) in TFA (40 mL) was added Ac₂O (6.30 mL, 66.9 mmol). The mixture was heated at reflux for 2 h. The solvent was removed by rotary evaporation. The solid was washed twice with diethyl ether (2 × 200 mL). Filtration and drying on high vacuum gave a white solid. This white solid was mixed with LiOH (1.70 g, 70.8 mmol) and dissolved in MeOH and water (1:1, v/v, 400 mL). The mixture was heated at 80 °C for 15 h. The solvent was removed by rotary evaporation. The crude solid was dissolved in water (60 mL) and treated with concd HCl (14 mL). The solid was obtained by filtration, dried on high vacuum, and then recrystallized with TFA (40 mL) and water (120 mL) to yield **5a** as a white solid (3.2 g, 2.65 mmol, 32%). Mp > 310 °C dec. IR (ATR, cm⁻¹): 1707 s, 1477 m, 1313 m, 1200 m, 964 m, 785 s. ¹H NMR (400 MHz, DMSO-*d*₆): δ 6.74 (s, 4H), 5.56 (d, *J* = 14.8 Hz, 2H), 5.46 (d, *J* = 14.8 Hz, 4H), 5.35 (d, *J* = 9.6 Hz, 2H), 5.25 (d, *J* = 15.6 Hz, 4H), 5.24 (d, *J* = 9.6 Hz, 2H), 4.65 (m, 8H), 4.13 (d, *J* = 15.6 Hz, 4H), 4.03 (d, *J* = 14.8 Hz, 4H), 4.03 (d, *J* = 14.8 Hz, 2H), 1.65 (s, 6H), 1.63 (s, 6H). ¹³C NMR (100 MHz, TFA, DMSO-*d*₆ as internal reference): δ 175.7, 157.0, 156.6, 149.5, 127.4, 113.7, 79.9, 78.3, 72.0, 71.4, 65.8, 53.2, 48.4, 35.0, 15.1, 14.3. HR-MS (ESI): calcd for C₇₀H₆₁N₁₆O₂₀ 1197.3622, found 1197.3548.

Compound 5b: A mixture of **4b** (2.90 g, 2.39 mmol), ethyl bromoacetate (3.20 g, 19.1 mmol), and anhydrous K₂CO₃ (6.62 g, 48.0 mmol) in MeCN (300 mL) was heated at reflux for 10 h. Solvent was removed under reduced pressure. Crude product was extracted with acetone (3 × 70 mL). After the solvent was removed with rotary evaporation, the crude product was washed with ethyl acetate (15 mL) to yield a white solid. And then this white solid was mixed with LiOH (0.400 g, 16.7 mmol) and dissolved in MeOH and water mixture (1:1, v/v, 120 mL). The mixture was heated at 80 °C for 15 h. Solvent was removed with rotovapory evaporation. The crude solid was treated with water (60 mL) and concd HCl (1.6 mL, 19.2 mmol) and then filtered to yield **5b** as a white solid (1.7 g, 1.2 mmol, 50%). Mp > 248 °C dec. IR (ATR, cm⁻¹): δ 1713 s, 1462 s, 1380 m, 1315 m, 1224 s, 1196 s, 1094 m, 971 s, 863 m, 801 m, 696 m. ¹H NMR (400 MHz, D₂O): δ 7.02–6.81 (m, 20H), 6.57 (s, 4H), 5.71 (d, *J* = 16.0 Hz, 4H), 5.58 (d, *J* = 15.2 Hz, 2H), 5.21 (d, *J* = 8.8 Hz, 2H), 5.09 (d, *J* = 15.2 Hz, 4H), 4.93 (d, *J* = 8.8 Hz, 2H), 4.31 (d, *J* = 15.6 Hz, 4H), 4.28 (d, *J* = 15.2 Hz, 4H), 4.18 (d, *J* = 15.6 Hz, 4H), 4.10 (d, *J* = 16.0 Hz, 4H), 3.99 (d, *J* = 15.2 Hz, 2H). ¹³C NMR (100 MHz, TFA, 1,4-dioxane as internal reference): δ 173.7, 157.5, 155.0, 148.0, 128.3, 128.04, 127.3, 127.1, 126.3,

(32) Haeg, M. E.; Whitlock, B. J.; Whitlock, H. W. *J. Am. Chem. Soc.* **1989**, *111*, 692–696. Couri, M. R. C.; Vieira de Almeida, M.; Fontes, A. P. S.; Chaves, J. D. A. S.; Cesar, E. T.; Alves, R. J.; Pereira-Maia, E. C.; Garnier-Suillerot, A. *Eur. J. Inorg. Chem.* **2006**, 1868–1874.

126.1, 125.4, 125.3, 112.4, 86.3, 85.3, 70.6, 69.6, 64.2, 52.2, 48.5, 35.3. HR-MS (ESI): calcd for $C_{70}H_{61}N_{16}O_{20}$ 1445.4248, found 1445.4252.

Acknowledgment. L.I. thanks the National Science Foundation (CHE-0615049 and CHE-0914745) for financial support.

Supporting Information Available: Synthetic procedures and characterization data for **4b** and **6**, direct and competitive binding titrations for determination of K_a values, 1H and ^{13}C NMR spectra for all new compounds, 1H NMR spectra of selected host-guest complexes of **5a**, and crystallographic information files for **5b**, **5b·20**, and **5a·25** (CIF). This material is available free of charge via the Internet at <http://pubs.acs.org>.